Journal of Power and Energy Engineering, 2024, 12, 1-19
https://www.scirp.org/journal/jpee
ISSN Online: 2327-5901
ISSN Print: 2327-588X

Simulation Study of Solid Rocket Motor C/C Throat Liner Ablation Based on Two Regions

Guanneng Chen, Yihua Xu*, Xiaojiang Zha, Hemeng Shi, Bing Liu

School of Aircraft Engineering, Nanchang Hangkong University, Nanchang, China
Email: *xiaotuanxia@qq.com

How to cite this paper: Chen, G.N., Xu, Y.H., Zha, X.J., Shi, H.M. and Liu, B. (2024) Simulation Study of Solid Rocket Motor C/C Throat Liner Ablation Based on Two Regions. *Journal of Power and Energy Engineering*, **12**, 1-19.
https://doi.org/10.4236/jpee.2024.124001

Received: March 11, 2024
Accepted: April 14, 2024
Published: April 17, 2024

Abstract

Based on the ablation micro-morphological characteristics, thermo-chemical ablation mechanism, and mechanical stripping mechanism, a dual-region solid rocket motor C/C throat liner ablation model and physical model are established. The ablation program was written and the experimental data of 70 lb BATES engine platform was used for model validation. The relative errors between the simulation calculation results and the experimental results were −6.83% - 10.20%. The ablation program was applied to study the effects of combustion chamber temperature, pressure, oxidation component concentration, throat particle concentration and particle scouring angle on the nozzle throat liner, which provides a reference for the design of the nozzle throat liner and the estimation of solid rocket motor ablation.

Keywords

Dual-Area Ablation Model, C/C Throat Liner, Ablation Environment, Ablation Program

1. Introduction

Solid rocket motors (SRMs) are widely used in aerospace and military applications because of their convenience and reliability. The Laval nozzle, as a key component of the SRM structure, in which the throat liner is the smallest diameter part of the nozzle, is subjected to high temperature, high pressure, high speed gas flow and erosive particles during engine operation, which results in damage to the throat liner and causes ablation of the inner surface. The occurrence of ablation will cause the retreat of the inner wall surface and size changes, which directly affects the engine thrust, speed and range and other overall performance indicators. Therefore, it is of great scientific and engineering significance to study the ablation pattern of throat lining to help understand the stresses

on key engine components, optimize the design, improve the performance, and ensure the operational safety [1].

Currently, C/C composites have become a widely used ablative thermal protection material in solid rocket motor nozzle design due to their excellent properties such as high strength, good ablative resistance, and very high impact resistance. The ablation of C/C composites is mainly divided into two aspects, namely, thermochemical ablation and mechanical ablation [2]. The former refers to the recession of the inner wall surface of the nozzle due to the oxidation reaction between the C surface and the oxidizing components (H_2O, CO_2, and OH) under the environment of high temperature, high pressure, and high speed gas flow [3]. The rate of which is determined by the kinetic rate of the heterogeneous reaction in conjunction with the rate of diffusion of the oxidizing components of the gas into the inner wall of the nozzle [4] [5]; whereas the latter is the result of the scouring of the gas flow under the effect of gas flow pressure, shear, and erosive particles, due to the different densities of the matrix and fibers, leading to ablation differences, which in turn cause granular spalling or flake spalling due to thermal stresses resulting in mass loss [6] [7].

Tharke *et al.* [8] proposed a minimum mechanism control model, which utilizes chemical kinetics and diffusion control to calculate the operating conditions separately, compares the values of the two regulating mechanisms, and takes the smaller value as its ablation rate, which synthesizes the effects of the chemical reaction rate and the gas diffusion rate on the ablation results.

Huang *et al.* [9] used a three-equation model to study the method of discriminating the thermochemical ablation control mechanism, and concluded that the discrimination of the nozzle ablation control mechanism should be determined by the content of H_2 in the gas in the nozzle and the activation energy of H_2 in the ablation environment. Zhang Bin *et al.* [10] proposed a new method to discriminate the ablation control mechanism based on the fact that the reaction of C with H_2O and CO_2 has different chemical reaction constants.

F. Ren, Sun H.S [11] and others in their study of surface exfoliation of carbon-based composites found that during thermochemical ablation, the matrix phase (carbon or graphitized matrix) and the reinforcing phase (carbon fibers) lead to different ablation recession rates due to the great difference in chemical properties, which leads to the change of the surface roughness, and the surface fibers protruding part of the surface when the surface roughness reaches the critical value under the pressure, air flow Shear stresses fail and spalling occurs.

In addition, Huang *et al.* [12] considered the erosion effect of particles independently by separating particle scouring from the gas-phase thermochemical ablation process when studying the erosion of the nozzle throat lining by particles generated by propellant combustion; Yin *et al.* [6] [7] [13] carried out the ablation experiments under the particle erosion conditions, revealed the mechanical stripping effect and thermochemical ablation influence of particles on the adiabatic layer and proposed a three-layer side model containing the base layer, the pyrolytic layer, ceramic layer, and scouring surface in a three-layer one-sided model; Yang

Sa [14] established a physical model of thermochemical ablation based on the void structure of the porous media layer, indicating that the distribution of porosity was controlled by the thermochemical ablation process, and the surface receded when the porosity of the ablated surface exceeded a critical value.

A common approach in engineering design is to estimate mechanical erosion rates from surface reaction rates using simple fitting functions, but the empirical parameters vary with conditions. The coupling of mechanical erosion and chemical reactions is rarely discussed, and the relationship between the two is not well defined.

In this paper, based on the ablation mechanism (thermochemical ablation and mechanical stripping) and model study and numerical simulation of C/C composites, it can be seen that the density difference between matrix carbon and fiber carbon of C/C composites, resulting in the volume depletion rate of matrix carbon is faster than that of charcoal fibers [11], which leads to the asynchrony of the two lines of ablation rate, and at the same time, under the influence of the diffusion concentration gradient of oxidizing components, the charcoal fibers present a shoot-shaped shape. which is assumed to be a porous Medium zone, the regional boundary to the temperature as a coupling condition, with the extension to the interior of the throat lining, the lack of oxidizing components makes the redox reaction can not be carried out, so as to maintain the original structural morphology, assumed to be the matrix area, the formation of the two zones as a whole. At the same time, comprehensive consideration of the material physical and chemical properties, heat and mass transfer, thermochemical ablation, airflow stripping, and particle erosion, the proposed establishment of the coupling of factors the dual-region solid rocket motor integrated ablation analysis model.

2. The Physical Model

2.1. C/C Body Ablation Model

According to the ablation structure of the C/C composite nozzle throat liner, a two-region body ablation model is established as shown in **Figure 1**, and the

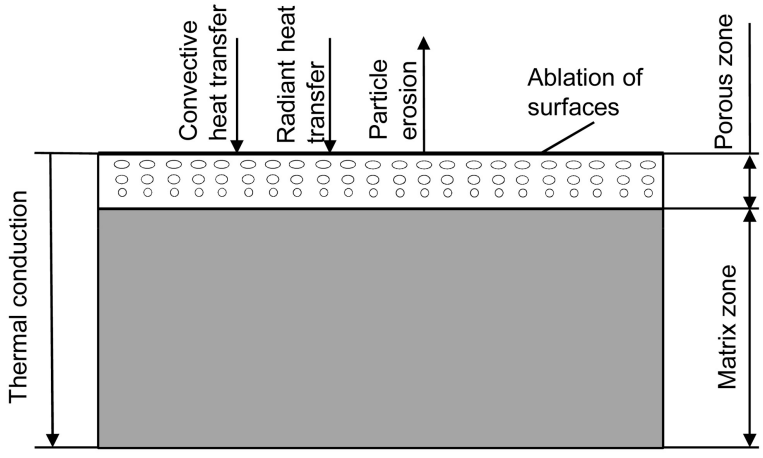

Figure 1. Schematic diagram of ablation model for C/C composites.

ablation area is divided into two parts: the porous medium area and the solid area, in which the porous medium area contains the thermally oxidized layer and the ablated surface layer, and the solid area refers to the C/C throat liner material matrix only.

In this model, T_w is the surface temperature of throat lining ablation, T_o is the critical temperature of thermo-oxidative reaction, and the ablation temperature of C/C composites is above T_o for the porous medium zone, and below it for the matrix zone. The ablation process of C/C composites throat lining is unsteady heat transfer, and the matrix zone needs to be analyzed for the heat conduction only [15]; in addition to thermo-chemical ablation within the porous medium zone, the heat and mass transfer of the thermal oxidative gas overflow as well as the ablation of the throat lining are also analyzed. heat transfer and mass transfer processes present in the attached surface layer; thermal oxidative ablation, gas stream stripping, particle erosion, heat conduction, heat radiation, heat convection, and heat increment caused by gas particles eroding the surface of the material on the ablated surface layer.

2.2. Heat and Mass Transfer

The ablation process of C/C composite throat lining are non-steady state heat transfer, only heat conduction in the matrix area needs to be analyzed; the porous media layer ablation thermodynamic force comes from the high-temperature gas inside the nozzle to the ablated material's thermochemical reaction, thermal radiation, convective heat transfer, and gas particles to erode the surface of the material brought about by the heat increment, in order to determine the heat flux into the ablated interior of the C/C throat lining, it is necessary to determine the thermo-chemical reaction heat flow, radiative heat transfer and convective heat transfer, where the thermochemical reaction heat flow [10] is

$$q_{chem} = \sum_{i=1}^{3} \frac{w_i}{M_i} \cdot \Delta H_t \tag{1}$$

where "w" denotes the mass consumption rate, M denotes the molecular weight of the component, ΔH_t denotes the standard enthalpy of formation for the reaction of C with component i, and i denotes the component, respectively; H_2O, CO_2, OH radiative heat transfer as:

$$q_{rad} = \varepsilon_{eff} \sigma \left(\left(T_g \right)^4 - \left(T_w \right)^4 \right) \tag{2}$$

where ε_{eff} is the effective radiation coefficient; σ is the Boltzmann constant; $\sigma = 5.698 \times 10^{-8}\ \mathrm{W} / \left(\mathrm{m}^2 \cdot \mathrm{K}^4 \right)$; T_g, T_w are the gas temperature and ablation surface temperature, respectively.

Convective heat transfer is:

$$q_{conv} = h_c \left(T_g - T_w \right) \tag{3}$$

where h_c is the convective heat transfer coefficient [13], calculated by the following equation [16]:

$$h = \frac{c}{D_t^{0.2}} \frac{\mu^{0.2} C_p}{Pr^{0.6}} \left(\frac{p_c}{c^*} \right)^{0.8} \left(\frac{D_t}{R_c} \right)^{0.1} \left(\frac{A_t}{A} \right)^{0.9} \sigma \tag{4}$$

where D_t is the nozzle throat diameter, μ is the gas viscosity coefficient, C_p is the gas constant pressure specific heat, Pr is the gas Prandtl number, p_c is the average pressure in the combustion chamber, c^* is the gas characteristic velocity, R_c is the radius of curvature of the nozzle throat, A_t is the channel area of the throat, A is the channel area at the computed cross-section of the throat lining, σ is the modification factor of convective heat transfer coefficient.

Under the action of two-phase flow, condensed-phase particles impacting the surface of the ablated material will produce heat increment to the generation, and after experimental analysis, the empirical equations for the calculation of the particle erosion heat flow regarding the erosion concentration, velocity, and scouring angle are derived [17]

$$\dot{q}_{mech} = 715956.7 \cdot n_p^{0.5} V_p^{0.18} \sin\theta \tag{5}$$

where $\dot{q}_{mech}$ is the particle erosion heat flow density (W/m^2), n_p is the erosion particle concentration (kg/m^3), V_p is the particle erosion velocity (m/s), and θ is the particle erosion angle.

2.3. C/C Oxidative Ablation Model

There are 6 main components in the gas stream at the ablation surface, which are: H_2O, CO_2, OH, CO, H_2, H, N_2 etc. Generally it is assumed that HCL, N_2 and Al_2O_3 don't react with the surface C(s), and at the same time, the components of the gas phase which don't take part in the reaction will be folded into the N_2, and as for the chemical reaction which may occur between the gas phases, taking into consideration of the fact that it is mainly carried out in mainstream, it is considered that it doesn't constitute ah to the surface ablation of the material. As for the possible chemical reaction between the gas phases, considering that it is mainly carried out in the mainstream, it is considered that it does not constitute a shadow ah to the ablation of the material surface.

From the Arrhenius equation, the reaction rate of each gas phase component is given by [8]:

$$k_i = A_i T_s^b \exp\left(-\frac{E_\alpha}{RT} \right) \tag{6}$$

The mass consumption rate in each gas phase reaction is;

$$w_i = k_i p_{iw}^n \tag{7}$$

Gas phase partial pressure;

$$P_{iw} = P_w P_{ie} \frac{M_w}{M_i} \tag{8}$$

The overall mass conservation is;

$$B' = \beta M_c \left(\frac{w_1}{M_1} + \frac{w_2}{M_2} + \frac{w_3}{M_3} \right) \tag{9}$$

where A_i and E are the frequency factor and activation energy, respectively, for the reaction of C with component i. R, T denote the molar gas constant and throat lining surface temperature, respectively. The relevant chemical kinetic parameters for these three reactions are listed in Table 1. The subscripts w and e denote the wall surface and outer edge, respectively. P and M denote the proportion of components and molecular weights of components, respectively. w denotes the mass production rate. B' and β are the two uncaused parameters. i denotes the components: H_2O, CO_2, OH, CO, H_2, H, N_2.

2.4. Airborne Corrosion

The gas stream stripping of carbon oxide layer in gas phase environment is complicated, and the influencing factors are: gas velocity, ambient pressure, high-temperature structural strength of the carbon oxide layer, viscous force generated by the escape of thermo-oxidized gas, and internal pressure. The detailed mechanism of these possible factors is still unclear, in addition to the high-temperature mechanical properties of the charcoal oxide layer, so it is not yet possible to judge the gas stream stripping of the charcoal oxide layer from the perspective of mechanical strength. However, the airflow exfoliation effect is described by the critical porosity, which suggests that exfoliation occurs once the porosity of the ablated surface layer reaches the critical porosity. The specific interpretation of the equation variables refer to

$$\varepsilon_c = 0.2 + 0.07 \times 0.896^{\tau} \tag{10}$$

When the shear force τ is greater than the structural shear strength τ_{cr}^{*}, the material undergoes airflow exfoliation.

2.5. Particle Erosion

In the engine throat gas contains a large number of energetic particles, in the process of work will occur on the surface of the C/C composite material erosion, particle erosion will aggravate the ablation rate of the C/C composite material. Erosion is mainly manifested in the heat increment brought about by high-temperature particles hitting the material surface, as well as the mass loss caused by mechanical stripping of the surface of the carbon oxide layer. The volume loss caused by a single particle to the material is in the form of shear loss Q_t due to tangential force and deformation yield loss Q_n due to normal force. The total erosion volume loss of a single particle, Q_s is a linear superposition of shear wear and deformation wear:

Table 1. Relevant chemical kinetic parameters.

Surface reaction	A_i	β	E/(J/mol)	n
$C + H_2O \rightarrow H_2 + CO$	1.5×10^3 [kg/(m²·s·Pa)]	0	2.9×10^5	0.5
$C + CO_2 \rightarrow 2CO$	28.3 [kg/(m²·s·Pa)]	0	2.8×10^5	0.5
$C(s) + OH \rightarrow CO + H$	3.57×10^{-3} [kg·K/(m²·s·Pa)]	−0.5	0	1

$$Q_s = Q_t + Q_n \tag{11}$$

The impact volume loss can be explained by the literature reference When the particle flow acts on the surface of the carbon oxide layer, a certain particle concentration is formed on the surface of the carbon oxide layer. When the eroded particle mass flux is ϕ_p, find the number of particles impinging on a unit area of the carbon oxide layer at a unit time N

$$N = \frac{\phi_p}{\rho_p K_p} \tag{12}$$

Translated with www.DeepL.com/Translator (free version) Define abbreviations and acronyms the first time they are used in the text, even after they have been defined in the abstract. Abbreviations such as IEEE, SI, MKS, CGS, sc, dc, and rms do not have to be defined. Do not use abbreviations in the title or heads unless they are unavoidable.

3. Mathematical Model

3.1. Underlying Assumption

On the basis of ensuring the correct principle, ignoring the secondary factors affecting the ablation performance of C/C throat lining material, the following assumptions are made on the ablation model of C/C throat lining material;

1) The ablation surface of C/C throat lining material in the throat of solid rocket ramjet is above the boundary layer of gas flow, and the heat conduction coefficient of C/C throat lining material is large, so the thermal expansion of C/C throat lining material is not taken into account.

2) The thickness of the ablation surface layer is very thin, so the ablation surface layer is approximated as a surface structure, in the C/C throat lining material ablation structure of the outermost layer of the grid; only consider the thermal effect of carbon oxidation, ignoring the internal heat conduction of the ablation surface layer.

3) The deposition of engine combustion chamber gas particles on the ablated surface of C/C throat lining material is not considered.

4) The gases involved in the ablation process are ideal gases.

5) In the C/C throat lining material ablation structure, and the ablation direction perpendicular to the plane of the ablation material, substrate, carbon oxidation layer and ablation surface layer of the structure and composition of the uniform. That is, C/C throat lining material ablation performance calculation according to the ablation direction parallel to the one-dimensional problem processing.

3.2. Ablation Calculation Area

In the ablation numerical calculation model, according to the shape and size of the ablation specimen of the throat lining, the solution area of the C/C composite is determined as shown in **Figure 2**, with a thickness H of 10 mm and a width L of 20 mm.

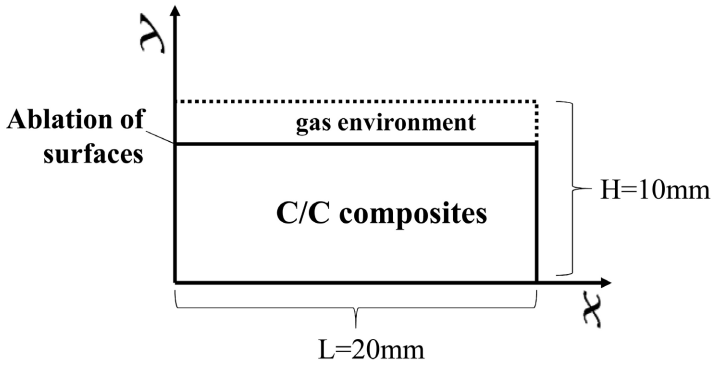

Figure 2. Ablation calculation area.

The dashed portion of in **Figure 2** indicates that after charcoal oxide stripping occurs, the ablated surface layer is pushed downward and the calculated area above is updated to a gas environment.

3.3. Regional Control Equations

3.3.1. Body Averaging Method

The volume averaging method is the main method to deal with complex flow heat transfer in porous media, which describes the flow and heat transfer processes in porous media from the microscopic level by establishing macroscopic conservation equations, and the volume averaging method is used in establishing the control equations for porous media. The volume averaging method is the basis for accurately deriving the macroscopic governing equations for flow and heat transfer in porous media from the microscopic equations. Taking a microelement containing gas and solid phases within a porous medium, as shown in **Figure 3**. Since the interfaces in the porous medium can move with time;

$$V = V_s(t) + V_g(t) \tag{13}$$

3.3.2. Harmonization of the Form of the Control Equations

In the solid region, only the heat transfer process exists, and a two-dimensional unsteady heat conduction equation is established. For the porous media region, which involves complex three-dimensional dispersive flow, the macroscopic conservation equations are established by the body-averaged method and the expressions of physical quantities are obtained. The ablation control equations for the throat lining of C/C composites contain a number of differential equations, and in order to facilitate the program to solve them, each of the differential control equations is unified into the form of a generalized equation

$$\zeta \frac{\partial(\rho\phi)}{\partial t} + \nabla \cdot (\boldsymbol{u}\rho\phi) - \Gamma\nabla^2\phi = S \tag{14}$$

For different differential control equations, the generalized unsteady coefficients ζ, the generalized diffusion coefficients Γ and the generalized source terms S in the generalized equations have their own specific forms.

For the porous medium energy equation, there are:

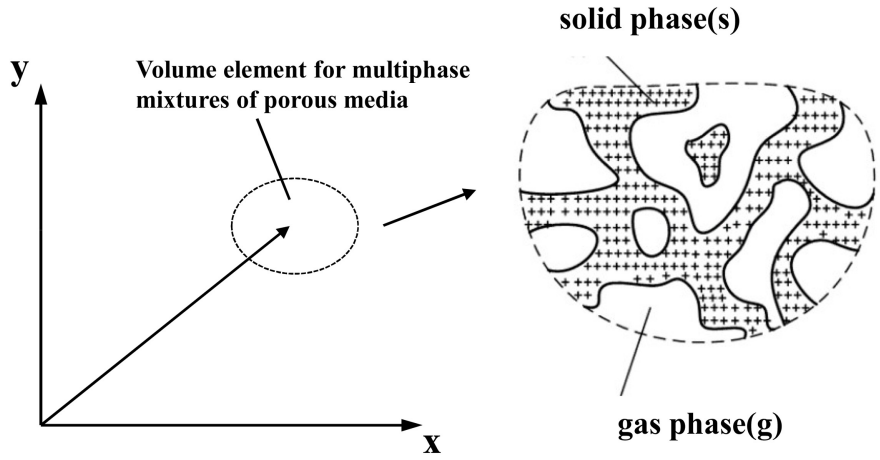

Figure 3. Schematic diagram of microelement of porous medium (carbon oxide layer).

$$\phi = T \tag{15}$$

$$\zeta = (1-\varepsilon)\rho_s c_s / \rho_g c_{pg} + \rho_g \tag{16}$$

$$\Gamma = (1-\varepsilon)\rho_s k_s + \varepsilon k_g / c_{pg} \tag{17}$$

$$S = \left(\varepsilon(1-\varepsilon)q_s'' + \varepsilon^2 q_g''\right) / c_{pg} \tag{18}$$

where the subscripts s and g denote the solid and gas phases, respectively; c is the specific heat of the solid; c_p is the specific heat of the gas at constant pressure, k the coefficient of thermal conductivity; and q'' is the heat per unit volume produced by the endothermic source (W/m^3).

3.4. Initial and Boundary Conditions

The initial temperature of the porous medium is given by the results of the temperature calculation at the previous moment, the initial pressure is set to the gas pressure, and the initial component concentration is set to the gas component concentration.

The upper boundary is in contact with the gas, and its temperature is determined by the gas thermal radiation, heat conduction, particle erosion heat gain and thermochemical ablation there:

$$-\lambda \left.\frac{\partial T}{\partial y}\right|_{y_p = y_{p\max}} = \dot{q}_{rad} + \dot{q}_{conv} + \dot{q}_{mech} + \dot{q}_{chem}$$

Initial concentration and pressure are available:

$$P\big|_{y_{p\max}} = P_c$$

$$Y_i\big|_{y_{p\max}} = Y_{c,i}$$

where P_c, $Y_{c,i}$ are the prevailing gas pressure and gas fraction respectively the lower boundary, *i.e.*, the interface between the porous medium and the substrate, is located at a position determined by the thermal oxidation reaction temperature T_s.

3.5. Numerical Processing Methods

The solid and porous media regions are solved using partitioned computation and boundary coupling methods, and the region boundaries are coupled with temperature as a coupling condition. In the computational region, the discretization is carried out using the interior node method and based on staggered meshing, and the control equations are discretized in a fully implicit format in order to ensure the stability of the numerical computation. The flow field parameters are solved using SIMPLE pressure algorithm modified to solve the algebraic equations using the alternating direction implicit iteration (ADI) method [18]. To ensure convergence of the iterative solution and avoid divergence, the successive subrelaxation iteration (SUR) method is used.

3.6. Bi-Regional Interface Treatment

Within each time step, the location of the charcoal oxidation surface is determined by temperature so that the solid region and the porous medium region are computationally solved separately and coupled in terms of temperature. This allows the intersection of the two regions to be determined, which in turn allows for iteration of the grid and data. Figure 4 demonstrates a schematic of the grid node changes for the before and after time steps when the charcoal oxidation surface is moved down.

The mesh division (y-direction) of the calculation region at the moment t is

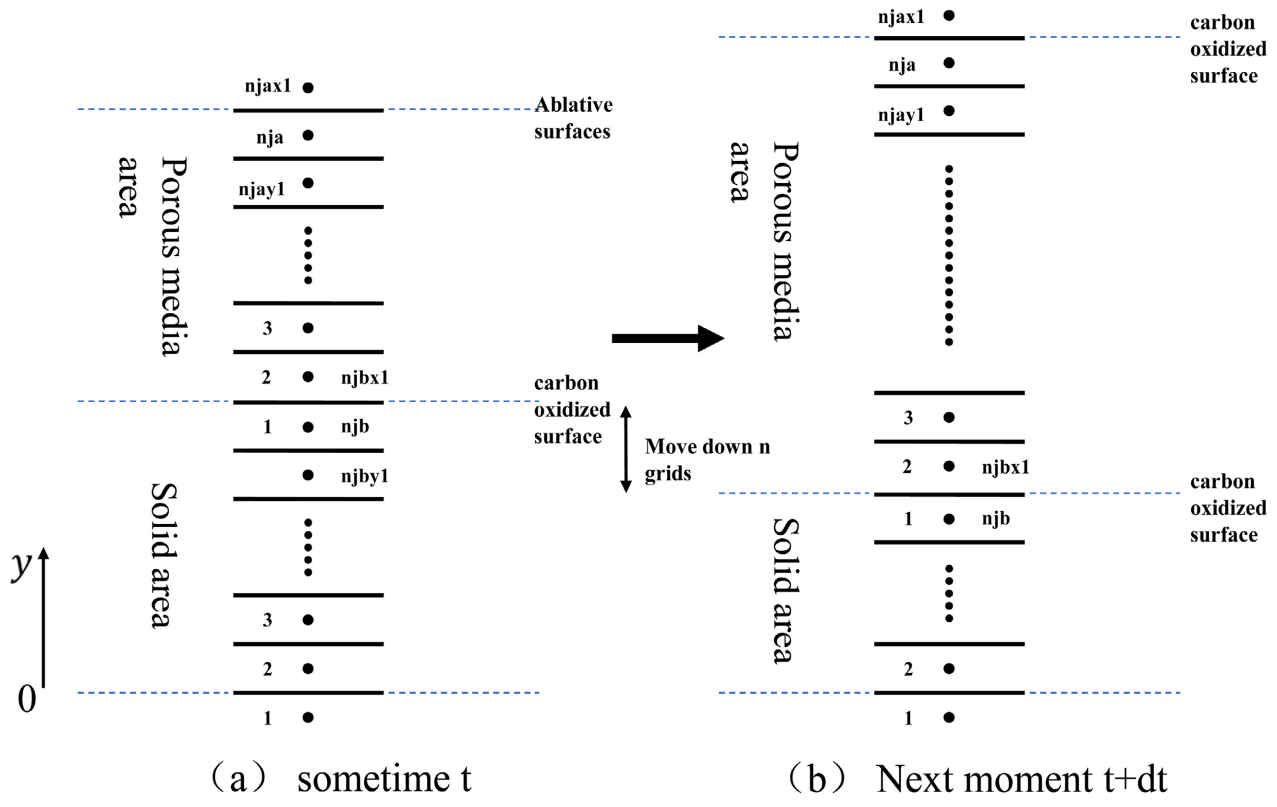

Figure 4. Change of mesh nodes at different moments when the thermal oxidation surface is moved downward.

shown in Figure 4(a). Firstly, each physical quantity in the porous medium region is calculated according to the boundary conditions, and the temperatures of the region's node 2 and node 1 are assigned to the solid region's nodes njbx1 and njb, respectively, and then the solid region undergoes the iterative calculation of heat conduction in order to obtain the temperature of the whole region. By comparing the junction temperatures with the thermal oxidation reaction temperatures, it is determined whether the interface between the two regions is downshifted or not. If it is downshifted, the mesh of the computational region needs to be re-divided. Figure 4(a) shows the meshing of the computational region (y-direction) at time t, while Figure 4(b) shows the re-gridding after the downward shift of the interfaces.

4. Analysis of Calculation Results

4.1. Ablation Model Validation

Geislert [15] summarized the last 40 years of Bates engine tests, focusing on the geometry of the 70-Pound Bates engine, the flow field components, and documented the pressure-time curves for the full range of engine operations and the ablation rates of the nozzle throat liners for different gas compositions. This subsection briefly discusses the computational results of the two-region body ablation model for C/C composites. In order to verify the reliability of the model, the study applies the model of this paper to simulate the ablation of five cases from the experimental data of Geisler based on the 70-lb BATES engine platform, with a computation time of 8 s. The inlet conditions of the five cases are shown in Table 2, and this data has been verified to be reliable [8] [19] [20], and Table 3 shows the remaining important parameters of the model.

As can be seen from Table 4 and Figure 5, the relative error between the ablation calculation results and the experimental results in the literature fluctuates from −6.83% to 10.20%, and the average absolute error is 6.296%, which is in

Table 2. Selected inlet conditions for Geisler simulation experiments.

Parameter	Case 1	Case 2	Case 3	Case 4	Case 5
P_d/Mpa	6.9	6.9	6.9	6.9	6.9
T_d/K	3580	3655	3715	3750	3745
Al	15%	18%	21%	24%	27%
Y_{H_2O}	0.145	0.105	0.07	0.045	0.025
Y_{CO_2}	0.04	0.025	0.015	0.005	0.0015
Y_{CO}	0.175	0.18	0.2	0.2	0.2
Y_{H_2}	0.02	0.02	0.02	0.02	0.02
Y_{HCl}	0.24	0.23	0.195	0.19	0.19
$Y_{Al_2O_3}$	0.28	0.34	0.4	0.44	0.47
Y_{N_2}	0.1	0.1	0.1	0.1	0.1

Table 3. Model parameters.

Parameter	Values
Material density ρ/(kg/m^3)	1830
Throat diameter D/mm	25.4
Specific heat C_S J/(kg·K)	1050
Heat conduction λ_s (W/m^2·K)	70
Rupture strength σ_{ys}/(Mpa)	24.7
Specific heat ratio y	1.135
Reaction heat q/kJ	125.6
Mach number Ma	1
Molecular mass M/(kg/mol)	30.008

Table 4. Comparison of calculated average ablation rate with experimental results.

Item	Case 1	Case 2	Case 3	Case 4	Case 5
Exp	0.353	0.284	0.2	0.124	0.069
Model	0.348	0.29814	0.18634	0.13665	0.07453
Error/%	−1.46%	4.98%	−6.83%	10.20%	8.01%

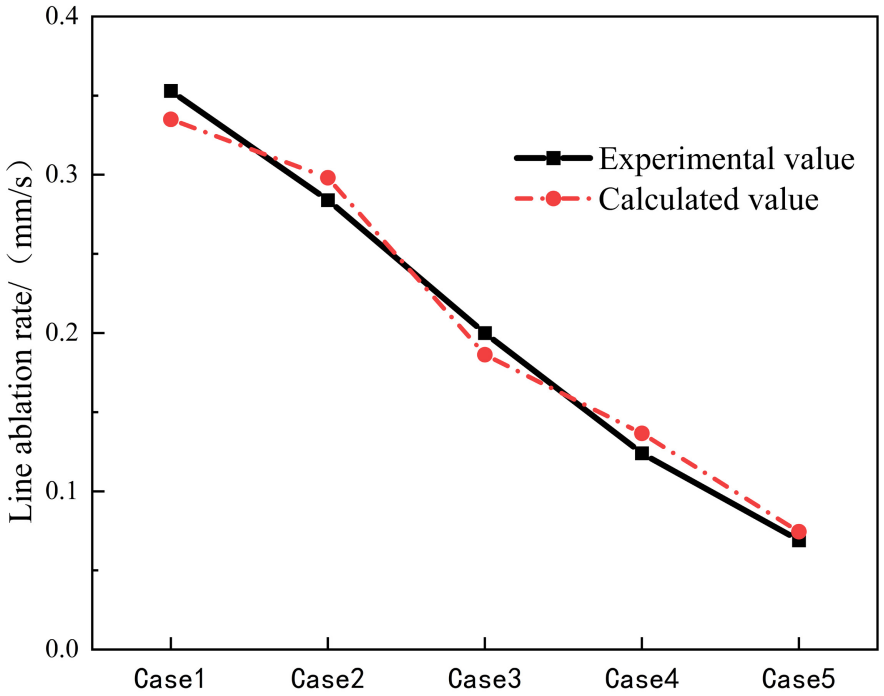

Figure 5. Comparison of ablation calculation results with experimental results.

line with the accuracy of the engineering calculations, which indicates that the model can more accurately simulate the ablation results of the nozzle liner of the C/C nozzle, and it has a high degree of reliability.

4.2. Effect of Environmental Parameters on Ablation

4.2.1. Effect of Combustion Chamber Temperature on Ablative Properties

With reference to the environmental parameters of the nozzle throat, 8 s ablation calculations are carried out with the ambient temperature as a variable, Figure 6, Figure 7 shows the temperatures are taken as 3000 K, 3327 K, 3480 K,

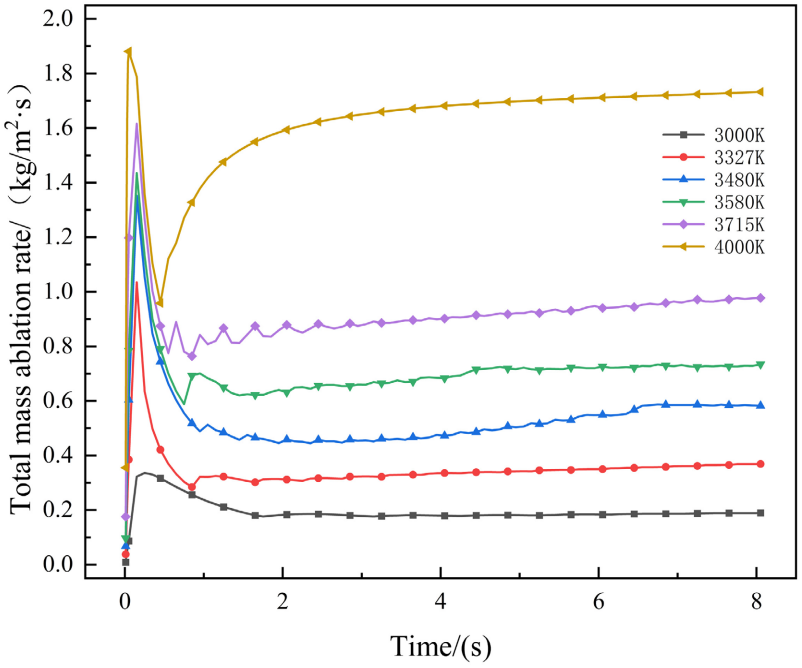

Figure 6. Variation of mass ablation rate with time at different temperatures.

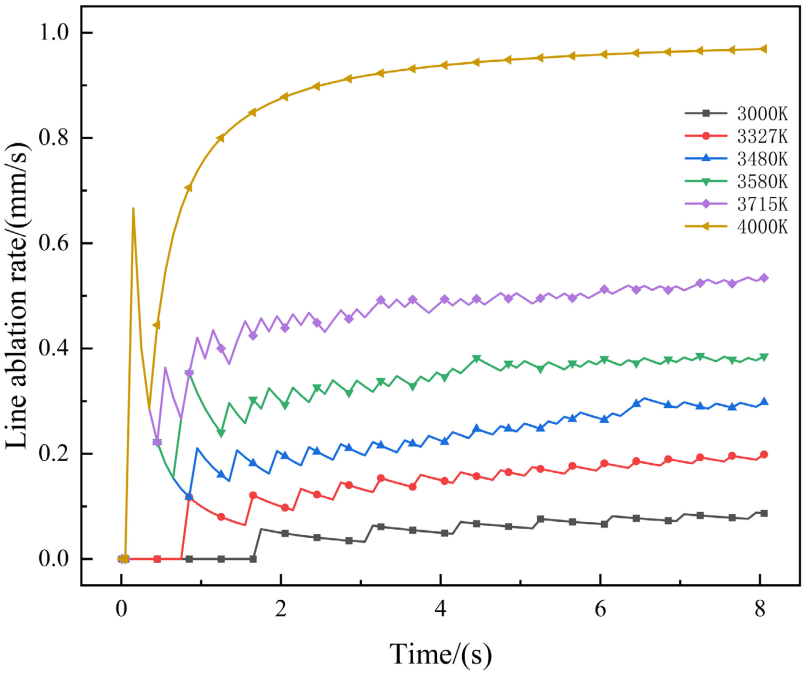

Figure 7. Variation of wire ablation rate with time at different temperatures.

3580 K, 3715 K, and 4000 K, respectively, in order to investigate the effect of the combustion chamber ambient temperature on the ablation of the C/C composites, and to calculate the line ablation rate and the total mass ablation rate of the C/C composites at different combustion chamber ambient temperatures. **Figure 8** shows the relationship between the total mass ablation rate, line ablation rate and ambient temperature at the end of throat ablation, from which it can be seen that the total mass ablation rate and line ablation rate increase as a function of the increase in combustion chamber temperature. The increase in ambient temperature will cause the boundary layer temperature rise, the fluid boundary layer transition from laminar to turbulent flow, the mass diffusion rate within the boundary layer will rise further, increasing the diffusion of oxidizing components in the gas, so that the reaction rate is controlled by the temperature to begin with, by the Arrhenius formula can be obtained from the temperature rises, the rate of thermo-oxidative reaction significantly faster, so that the mass ablation rate increases rapidly, and the loss of mass leads to the material The loss of mass leads to a larger porosity of the material, making it easier for gas stream stripping and particle erosion to take place, with a subsequent increase in the line ablation rate.

4.2.2. Effect of Combustion Chamber Pressure on Ablation Performance

Taking the average pressure of combustion chamber as a variable, to study the effect of combustion chamber pressure on the ablation performance of ablative materials, respectively, take the average pressure of combustion chamber as 4 MPa, 6.9 MPa, 8 MPa, 10 MPa, 12 MPa, 14 MPa. 8 s ablation calculations were carried out, and from **Figure 9**. We can get that the mass ablation rate and the

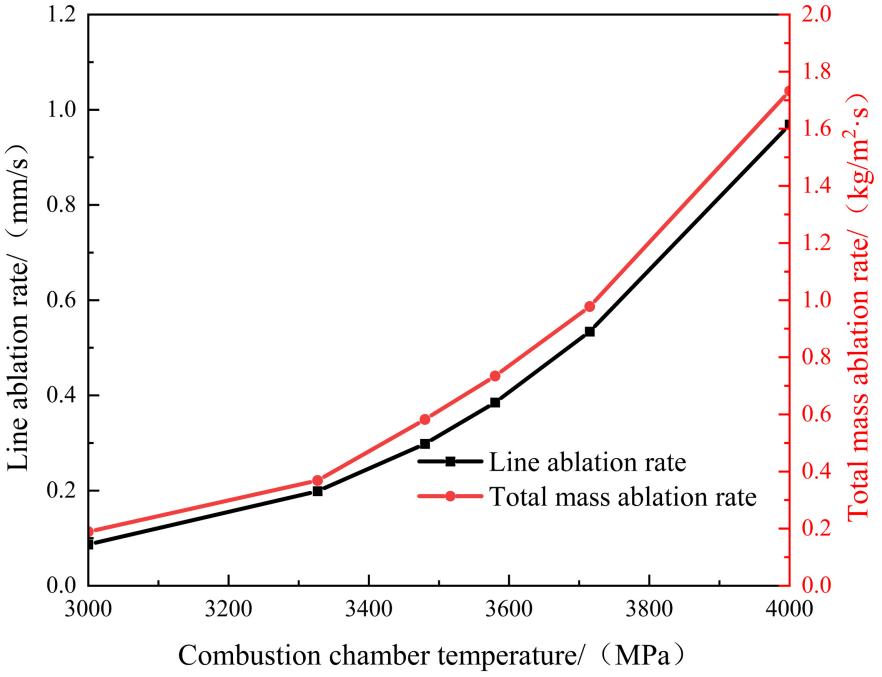

Figure 8. Total mass ablation rate, line ablation rate vs. ambient temperature.

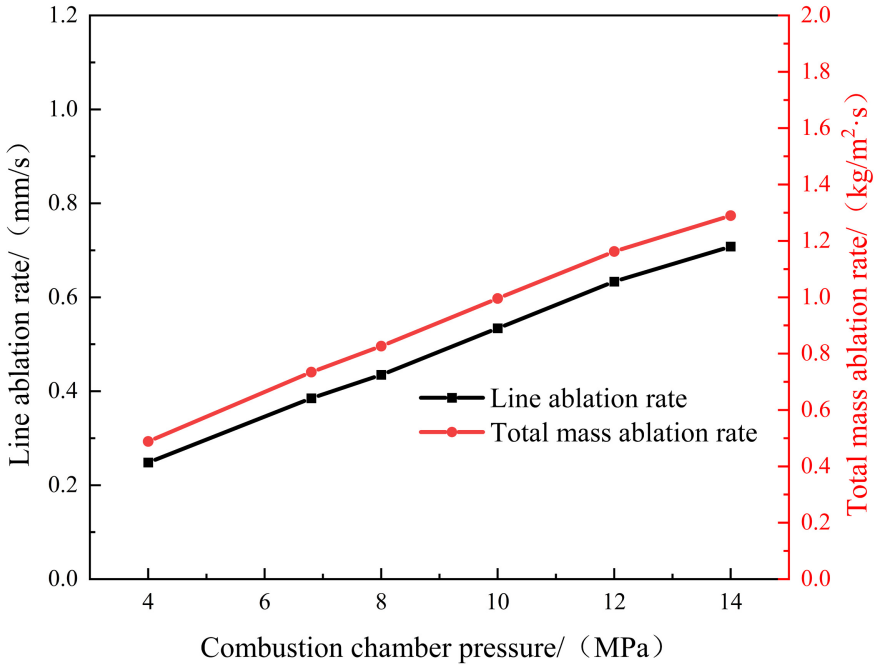

Figure 9. Total mass ablation rate, line ablation rate. combustion chamber pressure.

line ablation rate are all increasing linearly, and it can be seen that the pressure of combustion chamber is also an important factor influencing the performance of ablation. As the combustion chamber pressure increases, the nozzle flow density increases, convective heat transfer and mass transfer is enhanced; the flow Reynolds number increases, the boundary layer becomes thinner, and the resistance of heat transfer from gas to the wall and diffusion of oxidizing components to the wall decreases: the thermal oxidation reaction rate at the wall increases.

4.2.3. Effect of Oxygen Component Concentration on Ablation Properties

In order to investigate the effect of oxidizing gas content on the ablation performance of C/C composites, 8 s ablation calculations were carried out to calculate the mass ablation rate and linear ablation rate of the ablated material of the throat lining under the condition that the H_2O, CO_2 content varied in the range of 5% - 25%, respectively, taking the concentrations of H_2O and CO_2 to be 5%, 10%, 15%, 20%, and 25%, respectively. From the relationship between the total mass ablation rate, linear ablation rate and oxidizing gas content in **Figure 10**, it can be seen that as the concentration of oxidizing components increases, the concentration gradient becomes larger, the gas heat transfer to the wall, the oxidizing components to the wall diffusion rate accelerated, the oxidation reaction of the carbon oxide layer of the ablation rate increases, the rate of mass recession becomes faster, and the linear ablation rate and the total mass ablation rate show a clear trend of gradual increase.

When the oxidizing gas content is the same, with the increase of H_2O oxidizing gas content, the mass ablation rate and linear ablation rate of C/C composites

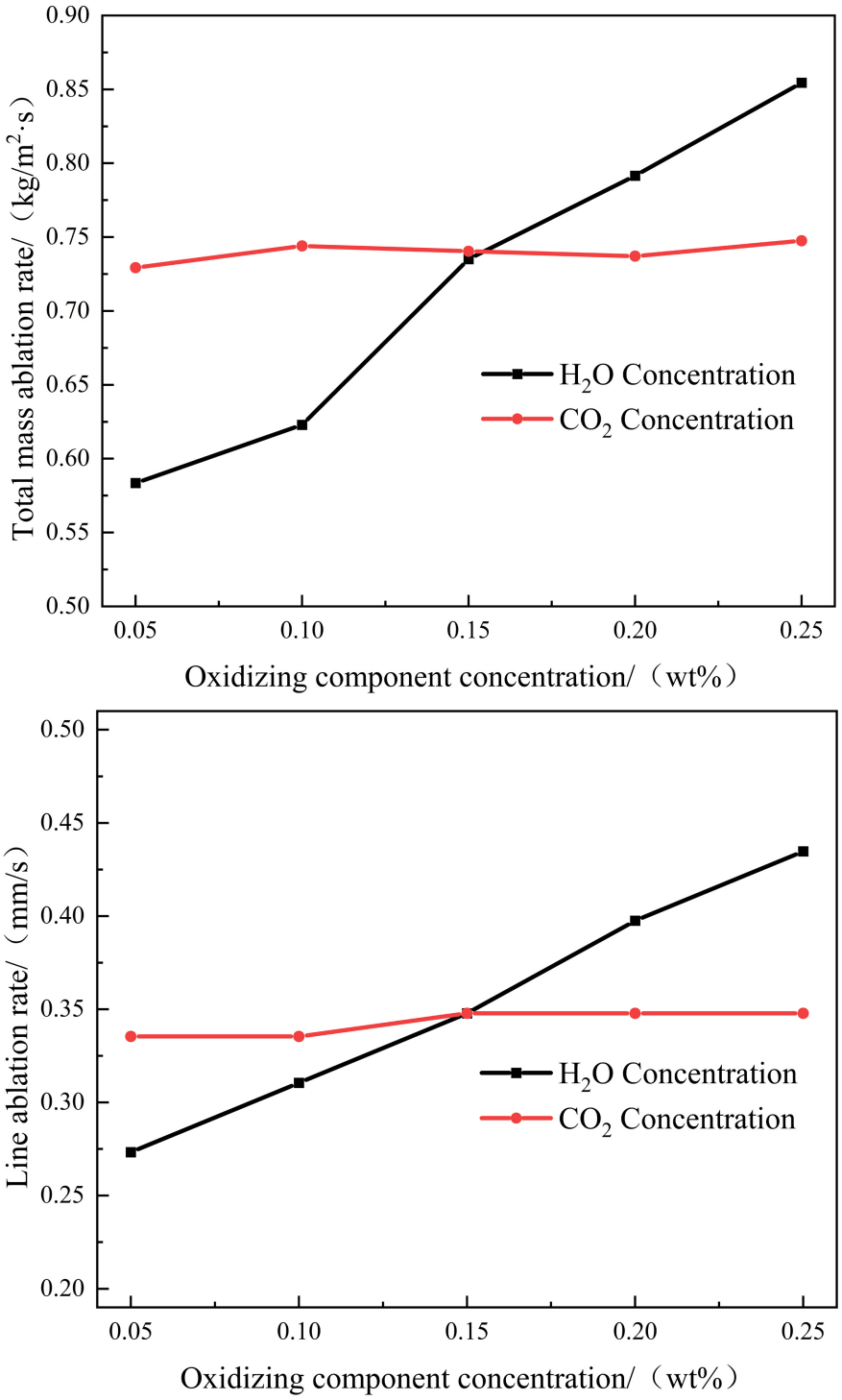

Figure 10. Total mass ablation rate, line ablation rate vs. concentration of oxidizing components H_2O, CO_2.

increase gradually, and the growth rate becomes larger gradually. With the increase of CO_2 oxidizing gas content, C/C composites mass ablation rate, line ablation rate increase is smaller; different oxidizing gases on the performance of the ablative material effect size: $H_2O > CO_2$.

5. Conclusions

On the basis of the classical nozzle throat thermal oxidation ablation model, the thermal oxidation minimum control mechanism model is selected to increase the influence of airflow stripping and particle erosion on the throat ablation, and due to the different physical problems contained in the two regions, the solid, porous media region partitioned computation and boundary coupling methods are adopted for the solution, and the regional boundaries are calculated using the temperature as the coupling condition. The ablation analysis model based on the two regions is established, and the model is verified to have high accuracy by the comparison of the experimental data of 70-lb BATES engine. Based on the model, the ablation process of the nozzle throat is calculated, and the influence of environmental parameters on the nozzle throat ablation is analyzed, and the main conclusions are as follows.

1) The ablation of C/C composite nozzle throat liner is mainly thermochemical ablation, and particle erosion and gas flow stripping account for a relatively small proportion.

2) The combustion chamber temperature not only affects the temperature distribution of the inner wall surface of the nozzle, but also has a direct effect on the concentration of the gas components and the chemical reaction rate of the inner wall surface of the nozzle. As the temperature of the combustion chamber rises, which leads to the difference of the thermochemical ablation rate of the inner wall surface of the nozzle, the mass ablation rate of the throat abrasion and the line abrasion rate are increased as a function of the temperature of the nozzle.

3) The change of the combustion chamber pressure directly leads to different pressure fields in the nozzle, with the increase of the combustion chamber pressure makes the gas to the inner wall of the nozzle heat transfer and oxidizing components to the wall surface of the diffusion enhancement, the chemical reaction rate also increases, so the throat ablation of the line ablation rate and mass ablation rate increases, and the two approximate and the pressure is proportional to the relationship.

4) nozzle wall surface oxidizing component concentration increases, the concentration gradient becomes larger, the gas to the wall heat transfer, oxidizing component to the wall diffusion rate accelerated, linear ablation rate and the total mass ablation rate showed a clear trend of gradual increase, and at the same time by the concentration of the oxygen component of the ablation rate of H_2O, CO_2 changes, can be obtained from the H_2O, is the main oxidizing component to determine the performance of the throat ablation.

Conflicts of Interest

The authors declare no conflicts of interest regarding the publication of this paper.

References

[1] Wang, L.W., Tian, W.P., Guo, Y.Q. and Lin, Z.Y. (2019) Progress of Solid Rocket Motor Nozzle Throat Liner Ablation. *Journal of Solid Rocket Technology*, **42**, 135-142+148. http://doi.org.10.7673/j.issn.1006-2793.2019.02.001

[2] Yan, Y. (1985) Combustion of HMX-CMDB Propellants. *Propellants, Explosives, Pyrotechnics*, **10**, 192-196. https://doi.org/10.1002/prep.19850100607

[3] Shimada, T., Sekiguchi, M. and Sekino, N. (2006) Numerical Analysis of Flow Inside a Solid Rocket Motor with Relation to Nozzle Inlet Ablation. 36*th AIAA Fluid Dynamics Conference and Exhibit*, San Francisco, 5-8 June 2006. https://doi.org/10.2514/6.2006-3891

[4] Kuo, K.K. and Keswani, S.T. (1985) A Comprehensive Theoretical Model for Carbon-Carbon Composite Nozzle Recession. *Combustion Science and Technology*, **42**, 145-164. https://doi.org/10.1080/00102208508960374

[5] Acharya, R. and Kuo, K. (2006) Effect of Chamber Pressure & Propellant Composition on Erosion Rate of Graphite Rocket Nozzle. 44*th AIAA Aerospace Sciences Meeting and Exhibit*, Reno, 9-12 January 2006. https://doi.org/10.2514/6.2006-363

[6] Yin, J., Xiong, X., Zhang, H.B. and Huang, B.Y. (2004) Research Progress of C/C Composites for Solid Rocket Motor Nozzle. *Materials Reports*, **18**, 46-48.

[7] Huang, H.M., Du, S.Y., Wu, L.C. and Wang, J.X. (2001) Analysis of Ablative Properties of C/C Composites. *Acta Materiae Compositae Sinica*, **18**, 76-80.

[8] Thakre, P. and Yang, V. (2008) Chemical Erosion of Carbon-Carbon/Graphite Nozzles in Solid-Propellant Rocket Motors. *Journal of Propulsion and Power*, **24**, 822-833. https://doi.org/10.2514/1.34946

[9] Huang, H.M., Xu, X.L. and Jiang, G.Q. (2009) Discrimination for Ablative Control Mechanism in Solid-Propellant Rocket Nozzle. *Science in China Series E: Technological Sciences*, **52**, 2911-2917. https://doi.org/10.1007/s11431-009-0274-2

[10] Zhang, B., Liu, Y., Wang, C.H., *et al*. (2010) New Discrimination Method for Ablative Control Mechanism in Solid-Propellant Rocket Nozzle. *Science China Technological Sciences*, **53**, 2718-2724. https://doi.org/10.1007/s11431-010-4081-6

[11] Ren, F., Sun, H.S. and Liu, L.Y. (1996) Theoretical a Analysis for Mechanical Erosion of Carbon-Base Materials in Ablation. *Journal of Thermo Physics Heat Transfer*, **10**, 593-587. https://doi.org/10.2514/3.834

[12] Huang, H.M., Xu, X.Q. and Jiang, G.Q. (2009) Discernment of Solid Rocket Nozzle Ablation Control Mechanism. *Science in China*, **39**, 1558-1563.

[13] Lee, T.T. (2012) Experimental Study of the Surface Regression Rate to the Heat Transfer. *Geoforum*, **43**, 772-783. https://doi.org/10.1016/j.geoforum.2012.01.003

[14] Yang, S., He, G., LI, J., *et al*. (2012) Modeling of EPDM Ablation in the Loose/Dense Structure of Carbonized Layers. *Journal of Aerospace Dynamics*, **27**, 1172-1178.

[15] Bianchi, D., Nasuti, F., Onofri, M., *et al*. (2011) Thermochemical Erosion Analysis for Chraphite/Carbon-Carbon Rocket Nozzles. *Journal of Propulsion and Power*, **27**, 197-205. https://doi.org/10.2514/1.47754

[16] Chen, L.B., Sun, N., Li, L.Y. and Zhang, B. (2022) Quantitative Analysis of High-Dimensional Uncertainty in Thermochemical Ablation of C/C Throat Linings. *National University of Defense Technology*, **43**, 258-267.

[17] Jiang, G. and Wang, S. (1990) Study on the Mechanism of Particle Heat Gain in Nozzle. *Solid Rocket Technology*, **2**, 18-22.

[18] Wang, S.X., Li, J., *et al*. (2016) Modeling of Two-Zone Body Ablation of EPDM In-

sulation Materials in Gas Phase Environment. *Propulsion Technology*, **37**, 378-385.

[19] Geisler, R., Beckman, C. and Kinkead, S. (2013) The Relationship between Solid Propellant Formulation Variables and Motor Performance. Proceedings of the 11th Propulsion Conference, Anaheim, 29 September-1 October 1975, 1199 p.

[20] Borie, V., Brulard, J. and Lengelle, G. (1989) Aerothermochemical Analysis of Carbon-Carbon Nozzle Regression in Solid-Propellant Rocket Motors. *Journal of Propulsion and Power*, **5**, 665-673. https://doi.org/10.2514/3.23204